Fundamental Journals
International Journal of Fundamental Physical Sciences (IJFPS) ISSN:2231-8186
IJFPS, Vol 4, No 3, pp 95-100, Sept , 2014 ***C. A. Fisher***
DOI:10.14331/ijfps.2014.330071
http://dx.doi.org/10.14331/ijfps.2014.330071

On the Schottky Barrier Height Lowering Effect of Ti_3SiC_2 in Ohmic Contacts to P-Type 4H-SiC

C. A. Fisher[1,*], M. R. Jennings[1], Y. K. Sharma[1], A. Sanchez-Fuentes[2], D. Walker[2], P. M. Gammon[1], A. Pérez-Tomás[3], S. M. Thomas, S. E. Burrows[2] and P. A. Mawby[1]

[1] School of Engineering, University of Warwick, Coventry, CV4 7AL, UK
[2] Department of Physics, University of Warwick, Coventry, CV4 7AL, UK
[3] Institut Català De Nanociència i Nanotecnologia, 08193, Bellaterra, Spain

E-mail: Craig.A.Fisher@warwick.ac.uk

(*Received Sep 2014; Published Sept 2014*)

ABSTRACT

In this paper, an experimental investigation into titanium (Ti) / aluminium (Al)-based ohmic contacts to p-type 4H-silicon carbide (SiC) has been presented. Electrical characterisation of the fabricated contacts showed that metal structures with an initial Ti layer yielded the lowest specific contact resistance (ρ_c), with a mean value of 3.7×10^{-5} Ω-cm^2 being achieved after annealing in argon (Ar) at 1000°C for 2 minutes. Transmission electron microscopy (TEM) analysis illustrated the epitaxial relationship between the 4H-SiC and the as-deposited Ti layer, and, in conjunction with energy dispersive X-ray (EDX) analysis, showed that after annealing a ~5 nm thick layer of Ti_3SiC_2 was present, epitaxially arranged with the 4H-SiC. X-ray diffraction (XRD) analysis showed that the presence of the Ti_3SiC_2 metallic phase was more prevalent in the samples with Ti as the initial metal layer annealed at 1000°C, which corresponded with lower specific contact resistance. Fitting of experimental data to a thermionic field emission (TFE) model allowed the Schottky barrier height to be extracted; it was found that the lowest Schottky barrier heights were more prevalent where the most intense Ti_3SiC_2 phases were observed during XRD analysis.

Keywords: 4H-SiC, ohmic contact, p-type, Ti_3SiC_2

DOI:10.14331/ijfps.2014.330071

INTRODUCTION

Due to its excellent electrical and thermal properties, the wide band gap semiconductor material 4H-silicon carbide (SiC) is widely expected to displace silicon (Si) for power electronics applications (Jennings et al., 2014). 4H-SiC holds particular promise for high voltage (several kV and above) applications due to its high critical electric field strength of ~3 MV/cm, which is approximately an order of magnitude higher than that of Si. Moreover, the higher thermal conductivity (~4.5 W/cm-K) and wider energy band gap (3.26 eV) of 4H-SiC compared to Si (both approximately three times greater) means that devices can be operated at higher current density and at higher ambient temperatures, making it an ideal semiconductor material to use for high power and high temperature electronics (Lanni, Ghandi, Malm, Zetterling, & Ostling, 2012). With Si devices seemingly at their limit in terms of voltage, current and operating temperature ratings, 4H-SiC has the potential for devices to overcome these limitations and enable more efficient and more reliable electronics systems, as well as opening up possibilities for new applications in the future (Buttay C, 2011).

Despite 4H-SiC offering a wealth of advantages over Si for high power and high temperature electronics applications, its full potential has not yet been realised due to several key issues. For high voltage applications, the use of bipolar devices, such as PiN diodes, bipolar junction transistors (BJTs), thyristors and Insulated Gate Bipolar Transistors (IGBTs) is necessary for realising low on-state power losses due to the conductivity modulation effect, which serves to lower the resistance of the thick drift region required for

blocking high voltages. However, material defects resulting in short carrier lifetimes (Miyazawa & Tsuchida, 2013) and forward voltage drift (Okamoto et al., 2013) continue to be a problem, thus hindering commercialisation of these devices. High temperature electronics applications, beyond the capabilities of the currently used silicon-on-insulator (SOI) technology (>300°C), are also envisaged to require the use of bipolar 4H-SiC technology, due to concerns with the gate oxide integrity of MOS-based devices and circuits at these temperatures (Ghandi et al., 2011). Moreover, when compared to CMOS, bipolar technology allows for simple implementation of temperature compensation, in addition to its potential for higher operating speeds (Lanni et al., 2012). A problem that continues to hinder the performance of bipolar 4H-SiC devices is the poor quality and stability of the ohmic contact to p-type material, the reasons for which are well reported (Fisher et al., 2012). However, it is widely accepted that ohmic contacts to p-type 4H-SiC based on titanium (Ti) and Al yield the lowest specific contact resistance (ρ_c) (Roccaforte et al., 2012), with values of ρ_c down to around 10^{-5} Ω-cm^2. Achieving a low ρ_c is crucial for minimising losses in power devices as well as enabling high frequency switching operation (Jennings et al., 2007). In order to obtain acceptable ohmic characteristics to p-type 4H-SiC, a high temperature annealing process, typically in excess of 950°C, is required. As reported in (Johnson & Capano, 2004), this annealing process results in alloy formation at the metal-semiconductor interface, which serves to lower the Schottky barrier height at the interface and thus reduce the resistivity of the ohmic contact. The particular alloy that was found to be responsible for the lowering of the Schottky barrier is Ti_3SiC_2; this is due to the trapping of an atomic carbon layer at the 4H-SiC/Ti_3SiC_2 interface, which assists conduction across the interface (Wang, Saito, Tsukimoto, & Ikuhara, 2012). However, when directly depositing this metallic compound onto p-type 4H-SiC, it was shown in (Buchholt et al., 2011) that ohmic behaviour was not attained, even after annealing at 950°C. As such, Al plays a crucial role in ohmic contacts to p-type 4H-SiC; it was reported in (Gao et al., 2007) that it helps form a liquid alloy that in turn promotes the reaction between Ti and 4H-SiC.

Because of the crucial role that Ti_3SiC_2 plays in realising ohmic contacts to p-type 4H-SiC, it is of practical interest to gain an insight into the processing conditions that promote the formation of Ti_3SiC_2, in addition to the relationship between the presence of Ti_3SiC_2 and the Schottky barrier height in ohmic contacts to p-type 4H-SiC. As such, in this paper, a range of Ti/Al-based metal contact schemes and annealing conditions have been investigated, in order to determine the optimum conditions for forming the Ti_3SiC_2 metallic phase. Transmission electron microscopy (TEM) in conjunction with energy dispersive X-ray (EDX) analysis has been employed in order to determine the atomic structure at the interface between the 4H-SiC and the metal contact, and x-ray diffraction (XRD) has been used to quantify the presence of metallic phases in the contact structures. Transfer length method (TLM) structures have been used to compare the electrical characteristics of the metal contacts, and finally, the Schottky barrier height of the fabricated metal contacts has been extracted by means of fitting to a thermionic field emission (TFE) model.

EXPERIMENT

This work was carried out on a 4" 4H-SiC n-type Si-face substrate cut 4° off-axis with a micropipe density of <1 cm^{-2}, with a p-type epitaxial layer of 0.5 µm thickness and >1x10^{19} cm^{-3} doping concentration. The epitaxial wafer was then laser cut into 8x8 mm square dies for p-type ohmic contact studies. The dies then underwent a solvent-based cleaning process consisting of acetone, isopropanol and methanol baths, each for 5 minutes. This was followed by an acid-based cleaning process consisting of 5% hydrofluoric acid (HF), Radio Corporation of America (RCA) standard clean (SC1), 5% HF, RCA SC2, Piranha and a final 5% HF. Dies were rinsed in deionised (DI) water between each cleaning step and after the final step, and dried using N_2. After the cleaning process, low-pressure chemical vapour deposition (LPCVD) was used to deposit a 1 µm thick layer of tetraethyl orthosilicate (TEOS) oxide, which served as a masking layer for defining the individual TLM mesas. The TLM mesas were realised by using a photolithography process based on S1818 photoresist, with the SiO_2 mask being patterned using reactive ion etching (RIE). After the SiO_2 etch, the photoresist was removed in acetone, then the 4H-SiC was etched to a depth of 750 nm using inductively coupled plasma (ICP) etching based on a SF_6 + O_2 chemistry. The remaining SiO_2 was then removed in dilute HF.

After the definition of the TLM mesas in the 4H-SiC, a second 1 µm thick layer of TEOS SiO_2 was deposited onto the dies, to serve as both a passivation layer and to define the TLM contact pad areas. The oxide was etched to a depth of ~800 nm using RIE, then the remaining ~200 nm was etched using 10:1 buffered oxide etch (BOE) solution. By using BOE to etch the TEOS SiO_2, exposing the 4H-SiC surface, damage of the surface from the RIE process was avoided, and the sidewall profile obtained from the BOE process facilitated subsequent easy metal lift-off due to the isotropic nature of the etch. Next, metal contacts were sputtered onto the 4H-SiC, and the unwanted metal (outside of the contact pad areas) was removed along with the photoresist using an acetone lift-off process. The metallised TLM structures were then annealed in a rapid thermal annealing (RTA) furnace in an argon (Ar) atmosphere. Finally, a 1 µm thick Al layer was deposited and patterned using a wet etch process so that it remained over the TLM contact pads, for current spreading during probing to the contact test structures. The TLM structure layout and associated dimensions for various contact pad spacings (d_n) are outlined in Fig 1. A detailed discussion of the equipment used for these fabrication processes is given by (Sharma et al., 2014).

Two different metal schemes have been investigated, Al/Ti/Al (100/100/10 nm) and Ti/Al/NiV (30/100/25 nm), with annealing temperatures ranging from 950°C to 1050°C. Nickel vanadium (NiV) was added to the second metal contact structure in order to promote the reaction between the 4H-SiC and Ti at lower annealing temperatures, which is beneficial for reducing the surface roughness of the contact structure (Gao et al., 2007). In order to electrically characterise the fabricated

metal contacts, an Agilent Technologies B1500A semiconductor parameter analyser has been employed, in conjunction with a four point probe station and heated chuck. All measurements have been performed under dark conditions, with two probes for force and two for sense. TEM analysis has been carried out using a JEOL 2000FX system, and, for the XRD analysis, a Panalytical X'Pert Pro MRD system has been used. Finally, the Panalytical High Score Plus and the 2013 ICDD powder diffraction database have been used to identify metallic compounds in the XRD analysis.

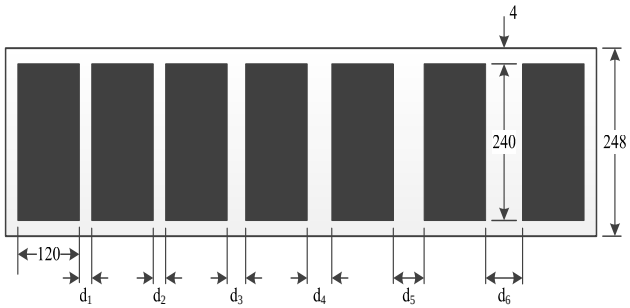

Fig. 1 Schematic diagram of fabricated TLM structures. Values for d_n are shown in the subsequent Figs.

RESULTS AND DISCUSSION

Electrical Characterisation

Fig 2 shows the total resistance as a function of contact spacing distance (d_n) for the Al/Ti/Al metal contacts across a range of annealing conditions. All measurements were performed at 25°C. It is noted that samples were also annealed at 950°C, but are not shown in this Fig as they exhibited rectifying characteristics. For each data point, a total of 12 TLM structures were measured, from which the mean values were calculated. It can be seen from Fig 2 that the samples annealed at 1000°C for 4 minutes exhibited the lowest mean specific contact resistance (ρ_c), at 5.8×10^{-4} Ω-cm^2. Annealing at the higher temperature of 1050°C was found to have an adverse effect on the specific contact resistance; in addition, increasing the annealing duration did not have a significant effect in reducing the specific contact resistance, as was observed at 1000°C. Fig 3 shows the corresponding total resistance as a function of contact spacing distance for the Ti/Al/NiV metal contacts across a range of annealing conditions, measured at 25°C.

Again, a total of 12 TLM structures were measured for each data point. It is evident that the extracted specific contact resistances are lower than the corresponding values for the Al/Ti/Al contacts, and ohmic behaviour has been attained at an annealing temperature of 950°C (albeit with a relatively high specific contact resistance of 1.6×10^{-3} Ω-cm^2). As with the Al/Ti/Al contacts, the lowest specific contact resistance was obtained at an annealing temperature of 1000°C, with a mean extracted value of 3.7×10^{-5} Ω-cm^2.

These results suggest that the Schottky barrier lowering metallic compounds at the metal-semiconductor interface are most effectively formed at 1000°C, and are formed more efficiently in the Ti/Al/NiV ohmic contacts.

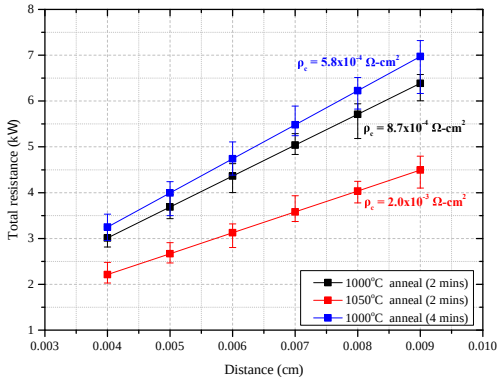

Fig. 2 Mean total resistance as a function of contact distance for Al/Ti/Al ohmic contacts across a range of annealing conditions. The extracted mean value of specific contact resistance is also outlined. Measurements were performed at 25°C.

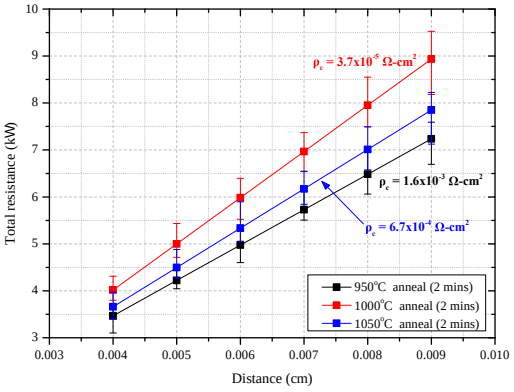

Fig. 3 Mean total resistance as a function of contact distance for Ti/Al/NiV ohmic contacts across a range of annealing conditions. The extracted mean value of specific contact resistance is also outlined. Measurements were performed at 25°C.

TEM Analysis

Fig 4 shows the crystal structure of the Ti/Al/NiV metal contact prior to annealing. It is evident that whilst the Ti has a crystalline structure, the Al is polycrystalline in nature. Due to the similar lattice constants of Ti and 4H-SiC (a = 2.95 Å and a = 3.07 Å respectively), the Ti is arranged epitaxially on the 4H-SiC; this is shown more clearly in Fig 5, which shows a high magnification TEM image of the 4H-SiC/Ti interface along with the fast Fourier transform (FFT) showing the corresponding hexagonal crystal structure of the 4H-SiC and the Ti.

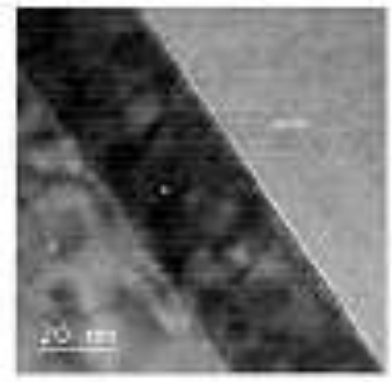

Fig. 4 TEM image showing the 4H-SiC/Ti/Al structure (as-deposited).

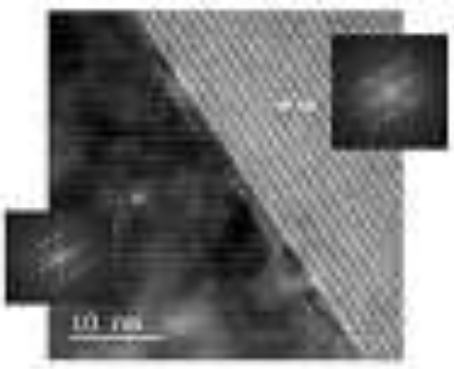

Fig. 5 TEM image showing the 4H-SiC/Ti interface and the FFT of the crystal structures (as-deposited).

Fig 6 shows the TEM image of the metal-semiconductor interface of the Ti/Al/NiV ohmic contact after annealing at 1000°C for 2 minutes. It is evident that the area of the Ti-rich layer in which the FFT was taken has a cubic crystal structure, though directly above the 4H-SiC there is a Ti-rich layer several nanometres thick, epitaxially arranged on the 4H-SiC.

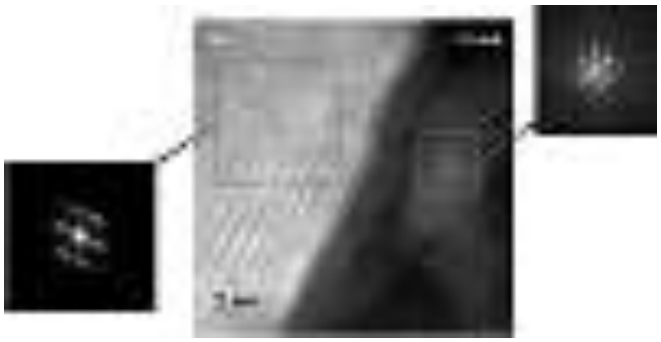

Fig. 6 TEM image showing the 4H-SiC/Ti-phase interface and the FFT of the crystal structures (annealed).

This layer is shown in greater detail in Fig 7. The *c* lattice constant of this layer has been measured to be 1.77 nm, indicating that it is the 321 MAX phase Ti_3SiC_2 (Ivanovskii & Enyashin, 2013).

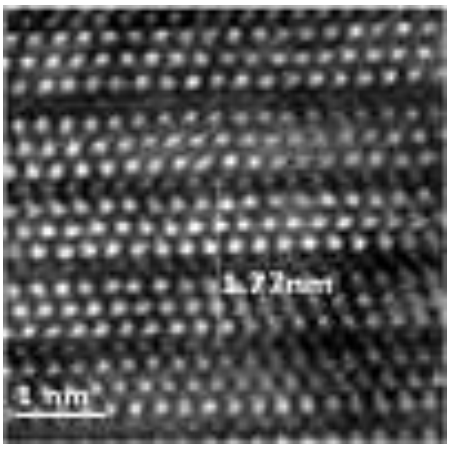

Fig. 7 STEM image showing the presence of Ti_3SiC_2 within the Ti-rich layer after contact annealing. The *c* lattice constant of the Ti_3SiC_2 phase has been measured and is also shown.

Though this was the most widely present Ti-Si-C phase identified in the TEM analysis, a mixture of MAX phases were observed, as well as the aforementioned cubic TiC compound. Some Al-rich areas were also observed, determined from the EDX analysis to be aluminium carbide.

XRD Analysis

Fig 8 shows the XRD spectra for the Al/Ti/Al metal contacts for the range of annealing conditions, as well as an as-deposited sample. It can be seen from the spectra for the as-deposited sample (black trace) that only peaks representing 4H-SiC, Al and Ti were present, and no metallic phases could be observed. However, after annealing at 1000°C for 2 minutes, the presence of Ti_3SiC_2 was detected (green trace).

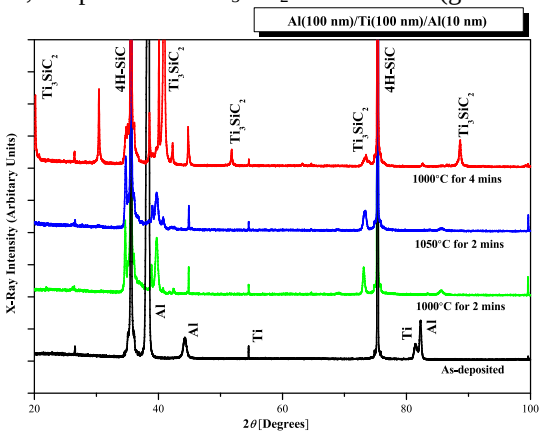

Fig. 8 XRD spectra of the Al/Ti/Al metal scheme for a range of annealing conditions.

In addition, other peaks were detected that could not be identified using the database. The sample annealed at 1050°C for 2 minutes (blue trace) exhibited a similar spectra to that of the sample annealed at 1000°C for 2 minutes, though with less intense peaks for the Ti_3SiC_2 metallic phase. However, the XRD spectra for the sample annealed at 1000°C for 4 minutes (red trace) showed a considerable departure from the previous samples, with much more pronounced Ti_3SiC_2 peaks.

Fig 9 shows the XRD spectra for the Ti/Al/NiV metal contacts for the range of annealing conditions. Though not shown in this Fig, it was found that the XRD spectra for the as-deposited sample showed that no metallic phases were present in the contact structure. It can be seen that the samples annealed at 950°C and 1050°C exhibit Ti_3SiC_2 peaks of relatively low intensity, although the XRD spectra of the sample annealed at 1050°C suggests slightly more formation of the metallic phase. As with the Al/Ti/Al metal scheme, the XRD spectra for the sample annealed at 1000°C shows an intense peak around 2θ = 40°, corresponding to the Ti_3SiC_2 phase. In addition, an intense peak representing Al_xNi_x is also evident in the sample annealed at 1000°C, which is considerably lower in the samples annealed at 950°C and 1050°C. From these XRD results it is clear that there is a correlation between the presence of Ti_3SiC_2 and the specific contact resistance of the metal-semiconductor contacts, with the lowest values of specific contact resistance being realised in the contact structures with a greater presence of Ti_3SiC_2.

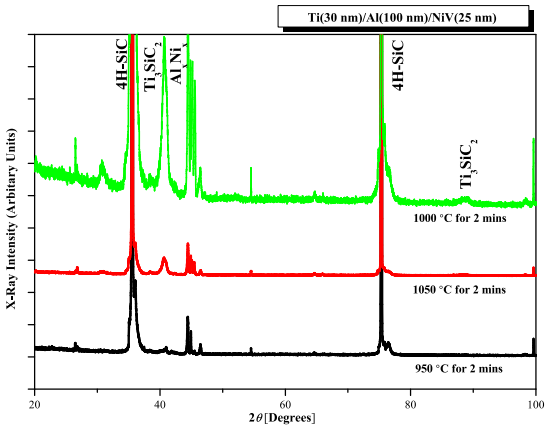

Fig. 9 XRD spectra of the Ti/Al/NiV metal scheme for a range of annealing conditions.

Extraction of Schottky Barrier Height

In order to quantitatively evaluate the Schottky barrier height lowering effect of Ti_3SiC_2 in each of the fabricated ohmic contact metal schemes, measurements to determine the dependence of the specific contact resistance as a function of measurement temperature have been performed. As outlined in (Iucolano, Roccaforte, Giannazzo, Alberti, & Raineri, 2007), this allows an insight into the current transport mechanisms to be obtained. The dominant current transport mechanism in a metal-semiconductor contact is dependent on the semiconductor doping concentration (N_A) and is related to a characteristic energy (E_{00}) described by (Yu, 1970),

$$E_{00} = \frac{h}{4\pi}\sqrt{\left(\frac{N_A}{m^*\varepsilon_S}\right)} \quad (1)$$

where h is Planck's constant, m^* is the effective hole mass and ε_S is the dielectric constant of 4H-SiC. For the doping concentration used in this work, it is expected that the dominant current transport mechanism is thermionic field emission (TFE) (Frazzetto, Giannazzo, Nigro, Raineri, & Roccaforte, 2011). Using the model for TFE presented in (Yu, 1970), the specific contact resistance can be expressed as a function of temperature, given by,

$$\rho_c = \left(\frac{kT}{qA^*}\right)\frac{kT}{\sqrt{\pi(\Phi_B + V_n)E_{00}}}\cosh\frac{E_{00}}{kT}\left[\sqrt{\coth\left(\frac{E_{00}}{kT}\right)}\right]e^{\left(\frac{\Phi_B+V_n}{E_0}-\frac{V_n}{kT}\right)} \quad (2)$$

where k is the Boltzmann constant, T is temperature, q is the electronic charge, A^* is the Richardson constant, Φ_B is the Schottky barrier height and V_n is the energy difference between the conduction band edge and the Fermi level. Finally, the parameter E_0 is given by,

$$E_0 = E_{00}\coth\left(\frac{E_{00}}{kT}\right) \quad (3)$$

When fitting to the TFE model, both Φ_B and N_A have been used as fitting parameters in order to extract the Schottky barrier height whilst accounting for possible departures from the specified value of N_A, due to imperfect doping control during epitaxial growth. Values of $\varepsilon_S = 9.7\varepsilon_0$ (where ε_0 is the vacuum permittivity), $A^* = 146$ A/cm^2-K^2 and $m^* = 0.91m$ (where m is the electron mass) (Frazzetto et al., 2011).

Fig 10 shows the specific contact resistance as a function of measurement temperature for the Al/Ti/Al ohmic contacts annealed at 1000°C for 4 minutes. In addition to the experimental data, the fit to this data using the TFE model is also shown. From this fit, a Schottky barrier height of 0.54 eV was extracted. Similarly,

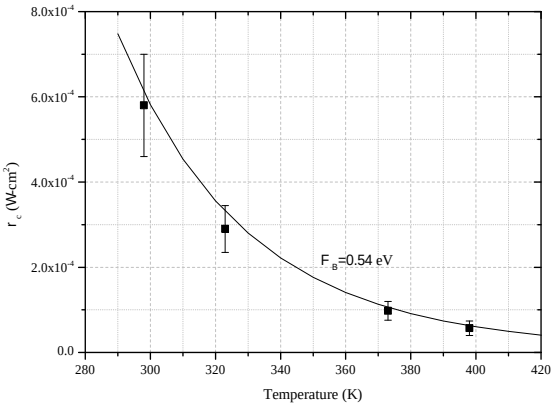

Fig. 10 Specific contact resistance as a function of measurement temperature for Al/Ti/Al ohmic contact annealed at 1000°C for 4 minutes. The solid line plot indicates the fit to experimental data.

Fig 11 shows the specific contact resistance as a function of measurement temperature for the Ti/Al/NiV ohmic contacts for the range of annealing conditions, as well as the fitted plots based on the TFE model. The extracted values of the Schottky barrier heights for each of the three annealing conditions are also shown, it can be seen that the Schottky barrier height drops from 0.56 eV for the sample annealed at 950°C to 0.43 eV for the sample annealed at 1000°C. On inspection of these results alongside the XRD spectra for the corresponding metal schemes, it can be seen that lower Schottky barrier heights (and lower specific contact resistances) are synonymous with the increased presence of Ti_3SiC_2; this is attributed to a more homogenous epitaxially arranged Ti_3SiC_2 layer at the metal-semiconductor interface, which facilitates current conduction across the interface (Wang et al., 2012). To the best of the authors' knowledge, this is the first time that this observation has been reported.

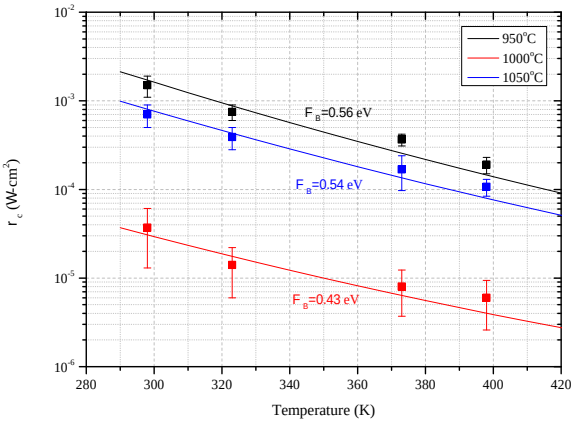

Fig. 11 Specific contact resistance as a function of measurement temperature for Ti/Al/NiV ohmic contacts for a range of annealing conditions. The solid line plots indicate the fits to experimental data.

CONCLUSION

In this paper, Ti/Al-based ohmic contacts to p-type 4H-SiC have been investigated. Electrical characterisation showed that that Ti/Al/NiV ohmic contacts yielded the lowest values of specific contact resistance, with a mean value of 3.7×10^{-5} Ω-cm^2 being achieved after annealing at 1000°C for 2 minutes. This was attributed to enhanced Ti_3SiC_2 formation due to the presence of Al and NiV in the metal contact structure. This value is similar to the lowest value of specific contact resistance reported elsewhere (Roccaforte et al., 2012). TEM analysis showed that when using Ti as the initial contact layer, it had an epitaxial arrangement with the 4H-SiC, arising due to their closely matched lattice constants. XRD analysis indicated that Ti_3SiC_2 was the predominant phase in the annealed samples, regardless of the initial metal deposition sequence, though was overall more significant in Ti/Al/NiV samples, with optimum formation of Ti_3SiC_2 being observed after annealed at 1000°C. The formation of Ti_3SiC_2 was found to correlate with Schottky barrier height lowering, and thus also with lower specific contact resistance; this was attributed to enhanced current conduction across the metal-semiconductor interface as a result of the epitaxial terraced structure of the Ti_3SiC_2 with respect to the 4H-SiC.

ACKNOWLEDGEMENTS

This research has been funded by the EPSRC grants EP/K035304/1 and EP/I013636/1, and has used cleanroom facilities funded by Advantage West Midlands and the European Regional Development Fund through the Science City Energy Efficiency project. The authors would like to thank Dr. Mark Crouch and the cleanroom staff for support during fabrication activities, and Mr Steven Hindmarsh for TEM sample preparation.

REFERENCES

Buchholt, K., Ghandi, R., Domeij, M., Zetterling, C.-M., Lu, J., Eklund, P., Spetz, A. L. (2011). Ohmic contact properties of magnetron sputtered Ti 3 SiC 2 on n-and p-type 4H-silicon carbide. *Applied physics letters, 98*(4), 042108-042108-042103.

Buttay C, P. D., Allard B, Bergogne D, Bevilacqua P, Joubert, Lazar M, Martin C, Morel H, Tournier D, Raynaud C. (2011). State of the art of High Temperature Power Electronics. *Materials Science and Engineering, B 2011; 176: 283-288*.

Fisher, C. A., Jennings, M. R., Bryant, A. T., Pérez-Tomás, A., Gammon, P. M., Brosselard, P., Mawby, P. A. (2012). *Physical modelling of 4H-SiC PiN diodes.* Paper presented at the Materials Science Forum.

Frazzetto, A., Giannazzo, F., Nigro, R. L., Raineri, V., & Roccaforte, F. (2011). Structural and transport properties in alloyed Ti/Al Ohmic contacts formed on p-type Al-implanted 4H-SiC annealed at high temperature. *Journal of Physics D: Applied Physics, 44*(25), 255302.

Gao, M., Tsukimoto, S., Goss, S., Tumakha, S., Onishi, T., Murakami, M., & Brillson, L. (2007). Role of interface layers and localized states in TiAl-based ohmic contacts to p-type 4H-SiC. *Journal of electronic materials, 36*(4), 277-284.

Ghandi, R., Buono, B., Domeij, M., Esteve, R., Schöner, A., Han, J., Ostling, M. (2011). Surface-passivation effects on the performance of 4H-SiC BJTs. *Electron Devices, IEEE Transactions on, 58*(1), 259-265.

Iucolano, F., Roccaforte, F., Giannazzo, F., Alberti, A., & Raineri, V. (2007). *Current transport in Ti/Al/Ni/Au ohmic contacts to GaN and AlGaN.* Paper presented at the Materials science forum.

Ivanovskii, A. L., & Enyashin, A. N. (2013). Graphene-like nano-carbides and nano-nitrides of transition metals. *Uspekhi Khimii, 82*(8), 735-746.

Jennings, M., Fisher, C., Thomas, S., Sharma, Y., Walker, D., Sanchez, A., Burrows, S. (2014). Physical and Electrical Characterisation of 3C-SiC and 4H-SiC for Power Semiconductor Device Applications *Physics of Semiconductor Devices* (pp. 929-932): Springer.

Jennings, M., Pérez-Tomás, A., Davies, M., Walker, D., Zhu, L., Losee, P., Covington, J. A. (2007). Analysis of Al/Ti, Al/Ni multiple and triple layer contacts to p-type 4H-SiC. *Solid-state electronics, 51*(5), 797-801.

Johnson, B. J., & Capano, M. A. (2004). Mechanism of ohmic behavior of Al/Ti contacts to p-type 4H-SiC after annealing. *Journal of applied physics, 95*(10), 5616-5620.

Lanni, L., Ghandi, R., Malm, B. G., Zetterling, C.-M., & Ostling, M. (2012). Design and characterization of high-temperature ECL-based bipolar integrated circuits in 4H-SiC. *Electron Devices, IEEE Transactions on, 59*(4), 1076-1083.

Miyazawa, T., & Tsuchida, H. (2013). Point defect reduction and carrier lifetime improvement of Si-and C-face 4H-SiC epilayers. *Journal of applied physics, 113*(8), 083714.

Okamoto, D., Tanaka, Y., Matsumoto, N., Mizukami, M., Ota, C., Takao, K., Okumura, H. (2013). *Development of High-Voltage 4H-SiC PiN Diodes on 4° and 8° Off-Axis Substrates.* Paper presented at the Materials Science Forum.

Roccaforte, F., Frazzetto, A., Greco, G., Giannazzo, F., Fiorenza, P., Nigro, R. L., Raineri, V. (2012). Critical issues for interfaces to p-type SiC and GaN in power devices. *Applied Surface Science, 258*(21), 8324-8333.

Sharma, Y., Xu, Y., Jennings, M., Fisher, C., Mawby, P., Feldman, L., & Williams, J. (2014). Improved Stability of 4H Sic-MOS Devices after Phosphorous Passivation with Etching Process. *International Journal of Fundamental Physical Sciences, 4*(2).

Wang, Z., Saito, M., Tsukimoto, S., & Ikuhara, Y. (2012). Terraces at ohmic contact in SiC electronics: Structure and electronic states. *Journal of applied physics, 111*(11), 113717.

Yu, A. (1970). Electron tunneling and contact resistance of metal-silicon contact barriers. *Solid-state electronics, 13*(2), 239-247.

